Fast and accurate approximate quasiparticle band structure calculations of ZnO, CdO, and MgO polymorphs

C. A. Ataide,* R. R. Pelá,† M. Marques, and L. K. Teles
Grupo de Materiais Semicondutores e Nanotecnologia (GMSN), Instituto Tecnológico de Aeronáutica (ITA), 12228-900 São José dos Campos/SP, Brasil

J. Furthmüller and F. Bechstedt
Institut für Festkörpertheorie und Theoretische-optik, Friedrich-Schiller-Universität, 07743 Jena, Germany
(Received 26 October 2016; published 17 January 2017)

We investigate ZnO, CdO, and MgO oxides crystallizing in rocksalt, wurtzite, and zincblende structures. Whereas in MgO calculations, the conventional LDA-1/2 method is employed through a self-energy potential (V_S), the shallow d bands in ZnO and CdO are treated through an increased amplitude (A) of V_S to modulate the self-energy of the d states to place them in the quasiparticle position. The LDA+A-1/2 scheme is applied to calculate band structures and electronic density of states of ZnO and CdO. We compare the results with those of more sophisticated quasiparticle calculations and experiments. We demonstrate that this new LDA+A-1/2 method reaches accuracy comparable to state-of-the-art methods, opening a door to study more complex systems containing shallow core electrons to the prize of LDA studies.

DOI: 10.1103/PhysRevB.95.045126

I. INTRODUCTION

Since the discovery of the light emitting diodes (LEDs) based on the group III nitrides, which enable blue emission [1], materials with potential application in ultraviolet opto-electronic devices have been investigated. In this context, technologies based on zinc oxide (ZnO) and related materials have emerged as a valuable alternative of great interest, as they allow us to meet demands for applications such as LEDs and photodetectors [1], semiconductor lasers in UV [2], flat screens [3], solar cells [4], sensors [5], and acoustical-optical devices [6], among others.

ZnO is a II-VI semiconductor with a wide band gap of 3.37 eV [7], which is very close to the value of the gap of GaN (3.30 eV) [8]. Band-gap engineering of ZnO can be achieved by alloying with cadmium oxide (CdO) in order to decrease the gap down to 0.84 eV [9,10] or with magnesium oxide (MgO) increasing the gap up to 7.7 eV [10,11]. Both CdO and MgO crystallize in the cubic rocksalt structure under ambient conditions, whereas ZnO crystallizes in the hexagonal wurtzite structure. However, rocksalt phases have also been found experimentally for ZnO and CdO under high-pressure conditions, and several others polymorphs have been predicted theoretically (for a review see Schleife *et al.* [11]). Therefore, polymorphism is an important property of these oxides, which influences drastically their electronic structures, and has to be addressed in the study of these ionic compounds.

From the theoretical point of view, the calculations of the electronic properties for the three oxides, specially ZnO and CdO, are challenging. Electronic structure calculations within the density functional theory (DFT) in its standard form within the local density approximation (LDA) [12] or the generalized gradient approximation (GGA) [13] for the exchange-correlation (XC) functional lead to significantly underestimated band gaps. Specifically in the case of the oxides, the gap predictions are even worse. For instance, the experimental fundamental band gaps of wurtzite GaN and ZnO are similar, 3.30 and 3.37 eV, respectively, but within DFT-LDA the predicted GaN energy gap is 2.0 eV, whereas for ZnO it is only 0.8 eV. According to Schleife *et al.* the ZnO gap is impaired by the overestimated pd repulsion [11]. Consequently, the use of pure standard DFT calculations to study electronic properties of ZnO-based systems have a great potential to produce wrong conclusions due to too high-lying valence Zn3d states (5.0 eV [11]) in comparison with the experimental data (7.3–8.8 eV [14–21]), whereas Ga3d electrons have binding energies larger by about 10 eV.

Moreover, the difficulties are not restricted to the standard DFT; even the well tested and successful hybrid functional approaches [22,23] or the highly sophisticated XC self-energy calculations within Hedin's GW approximation [24–26] do not agree with experiments at the same level of accuracy compared with their applications to other important compounds as GaAs or Si.

Particularly, the hybrid XC functionals [27], including the frequently used and well tested HSE03 or HSE06 ones of Heyd, Scuseria, and Ernzerhof [22,23], are not so accurate in the case of these oxides. The HSE06 calculation of ZnO provides an energy gap of 2.5 eV and a d band position of 6 eV with respect to the valence band maximum (VBM), both underestimated in comparison with experimental data [28]. When it comes to MgO, its large band gap presents a challenge to the HSE calculations, which still underestimate the band gap significantly [27]. The ideal mixing parameter is expected to vary inversely with the dielectric constant [29]. Therefore the default mixing parameter, 0.25, seems to capture only the physics of the screening in materials with small or medium-sized band gaps.

The calculation of the gaps of these oxides is also a challenging task for the GW approach [27,30–35], which

*ataidecaa@gmail.com
†Also at: Humboldt-Universität zu Berlin, Institut für Physik and IRIS Adlershof, Theoretische Festkörperphysik, Zum Großen Windkanal 6, 12489 Berlin, Germany.

may require some degree of self-consistency [35]. Indeed, different GW results for band gaps and the position of d bands may arise depending on the numerical treatment of the quasiparticle approach: (i) the starting point, (ii) degree of self-consistency, and (iii) the effort put on numerical convergence (which is usually slow). The simplest GW approach is a G_0W_0 [35] calculation using results of DFT calculations as the starting point. Historically the use of GW on top of LDA, G_0W_0@LDA, or PBE, G_0W_0@PBE, leads to the underestimated energy gaps: 2.1 eV or 2.5 eV for ZnO [26,36,37], 7.25 eV [38] and 7.42 eV [39] for MgO, and 0.43 eV and 0.21 eV [40] for CdO. Moreover, these calculations also give a too high d band position. A way to circumvent this problem is to consider another starting point, as a calculation with a hybrid XC functional [27]. In the case of MgO, G_0W_0 calculations performed on top of the HSE functional improves the situation [41], the predicted band gaps of 7.47 eV agrees well with the measured one, 7.7 eV [11]. An improvement is also achieved within G_0W_0@HSE03 calculations which provide for CdO an energy gap of 0.81 eV and a d band position of 8.4 eV, both in good agreement with experiments [41]. Also, the same method gives for ZnO an energy gap of 3.2 eV and a position of the d band of 6.96 eV, both in good agreement with experimental data [41], despite the numerical convergence being low and the calculation having a large computational demand due to both GW and HSE calculations. More recently, in order to reduce the computational cost of HSE calculations, another approach was proposed by Shih *et al.* combining GW and LDA+U [31], also leading to good results in comparison to experimental data, but still having a considerable computational cost due to the GW calculation. In this sense, a fast and accurate method for obtaining the band structure for these oxides is of great importance and could open an avenue for studying more complex systems.

In this work, we demonstrate that for ZnO, CdO, and MgO it is possible to obtain an electronic structure including approximate quasiparticle corrections. We employ the LDA-1/2 method, which includes self-energy corrections in a simplified way [42] and has a similar computational cost to standard DFT calculations. Its low cost makes it possible to include the spin-orbit interaction in all calculations. For the treatment of shallow d levels as in ZnO and CdO we generalize the standard LDA-1/2 method to better describe the position of the d states, by including the semicore states in the simulation of the self-energy potentials. As a progress of the methodological development we provide not only more accurate energy gaps, but also give a global improvement of the band structures. For all studied compounds, the calculations are performed for three hexagonal or cubic polymorphs, the wurtzite (WZ), rocksalt (RS), and zincblende (ZB) structures. We directly compare the band structure parameters as energy gap and position of cation d band when experimental data are available and predict approximate quasiparticle electronic bands for structures for which no experimental data are available.

II. METHODOLOGY

A. DFT and geometries

The structural properties are obtained using the DFT-LDA method [12]. In all calculations, to solve Kohn-Sham (KS) equations, we employ the projector-augmented wave (PAW) method [43], as implemented in the VASP code [44]. The outermost s, p, and d (in Cd and Zn) electrons are treated as valence electrons in our calculations. The Brillouin-zone (BZ) integrations are carried out with a set of $8\times8\times8$ k points, using the Monkhorst-Pack scheme [45]. To obtain the electronic density of states (DOS) we increase the k-point grid to $25\times25\times25$ and $14\times14\times14$ for cubic and hexagonal structures, respectively. The number of plane waves is limited by a cutoff of 800 eV.

B. LDA-1/2 method

All the electronic structures obtained within the LDA-1/2 method [42] include spin-orbit coupling (SOC) [46]. The LDA-1/2 method is described in detail in Refs. [42,47]; in this work we present the underlying physics of the method. The basic idea of the LDA-1/2 method is the Slater transition technique (STT) [48], in which the half occupied atomic eigenvalue is equal to the negative value of the ionization potential. This equality can be simply deduced combining Janak's theorem [49] and the empirical verification that the KS-eigenvalue varies approximately linearly with its own occupation. STT can be easily tested in atoms providing excellent agreement for calculated ionization potentials with experimental data [42]. The STT approach can be basically understood as the subtraction of the self-energy of the hole, which leads to approximate quasiparticle corrections. The physical meaning of this self-energy is not that one that arises in many-body perturbation theory [35], but it is in fact the energy necessary to localize the quasiparticle [42,47]. In the atom the application of this technique is straightforward since the subtraction of an electron of the system is possible. However, this is not the case of the solid, because it is very difficult to find a way to implement half ionization as the hole tends to be infinitely extended in a Bloch wave state.

In order to circumvent this problem, the half occupation is implemented in an infinite system by a modified potential, which is generated by the difference between two atomic potentials: one relative to Z electrons (Z being the atomic number of the chosen atom) and the second relative to Z-1/2 electrons. The result of this subtraction is a potential due to 1/2 electron, that we call self-energy potential V_S. V_S is subtracted from the local part of the Kohn-Sham potential in each self-consistent step, simulating the half occupation. Therefore, in this scheme there is no change in the number of electrons of the system, and although the eigenvalue related to the half hole is simulated by V_S, it is always fully occupied keeping the neutrality of the system. However, in practice there is a problem with adding this potential to all the atoms of an infinite crystal: The potential will diverge. V_S is a potential of an excess charge of 1/2 proton and has a tail of $0.5e^2/r$ (where r is the distance from the proton). Therefore the tail has to be trimmed by a step function. The final form of V_S is:

$$V_S(\vec{r}) = A\,\theta(\vec{r},CUT)\left[V^{Z}_{\text{atom}}(\vec{r}) - V^{Z-f}_{\text{atom}}(\vec{r})\right], \qquad (1)$$

where the coordinate origin is taken in the position of the atom, A is an amplitude of the potential (usually equal to 1), $\theta(\vec{r},CUT)$ is the steplike function (in practice approximately 1 for a radius smaller than the CUT radius and approximately

0 for a radius higher than CUT), and $V^{Z}_{\text{atom}}(\vec{r})$ is the atomic potential for Z electrons and $V^{Z-f}_{\text{atom}}(\vec{r})$ the atomic potential for $Z-f$ electrons, where the fraction of electrons f is usually equal to $1/2$. For nonmetallic solids the CUT parameter is optimized to maximize the fundamental gap [42,47].

The implementation of the STT concept to the case of infinite solid systems is what is called LDA-$1/2$ method. As in the atoms STT is directly related to ionization potentials of a certain level, its employment to calculate energy gaps has to deal with the calculation of the half occupied valence band maximum (VBM) and also the half occupied minimum of conduction band (CBM). Based on this idea of the self energy potentials to obtain the energy gaps, a half electron is subtracted (added) for the atomic orbital that characterizes the VBM (CBM). This initially general approach can be simplified considering only the correction of the VBM, which can be justified by the fact that conduction states are much more delocalized leading to negligible contributions to self-energy correction. Therefore, the LDA-$1/2$ receipt is in the majority of cases straightforward. For example, in the case of the III-V semiconductor AlN the $1/2$ electron is subtracted from the p orbital of the anion, the N atom, that totally characterizes the AlN VBM [47,50]. However, there are some cases in which the decision, which atom has to be ionized, is not straightforward, because the VBM may not be a pure p state of the anion, but may have some character of d or p states of the cation. In the cases of ZnO and CdO, the presence of d cation character in the VBM cannot be neglected, therefore, this fact will be taken into account in the generalized model.

The LDA-$1/2$ method essentially results in gap corrections for many semiconductors and insulators. In principle, one does not expect an improvement of the dispersion of other bands far away from the energy gap region, compared with respective DFT bands. However, the cases of ZnO and CdO are more complicated, because there is a clear influence of semicore levels close to the gap region. It is well known that the cation d states in ZnO and in CdO calculated with standard DFT give rise to artificial high-lying semicore bands

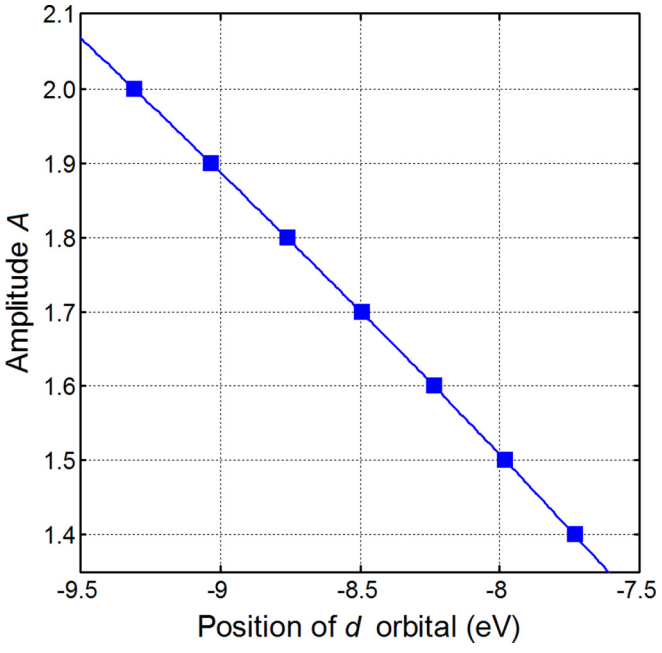

FIG. 1. Plot of the amplitude A vs the d state position below VBM. This plot refers to WZ ZnO.

TABLE I. VBM character analysis using LDA and the LDA+A correction for ZnO, CdO, and MgO in WZ, RS, and ZB phases. All values are expressed in percentage.

Struct.	Method	Orbital	Zn	O	Cd	O	Mg	O
RS	LDA	p	0.0	66.5	0.0	76.2	2.5	97.6
		d	33.5	0.0	23.8	0.0	0.0	0.0
	LDA+A	p	0.0	84.5	0.0	85.6		
		d	15.5	0.0	14.4	0.0		
ZB	LDA	p	2.4	63.5	1.8	74.9	1.2	94.5
		d	34.1	0.0	23.3	0.0	4.3	0.0
	LDA+A	p	2.6	84.5	2.1	83.5		
		d	16.8	0.0	14.4	0.0		
WZ	LDA	p	2.5	63.5	2.1	73.6	0.8	96.1
		d	34.7	0.0	24.3	0.0	3.2	0.0
	LDA+A	p	2.6	80.8	2.5	82.8		
		d	16.7	0.0	14.8	0.0		

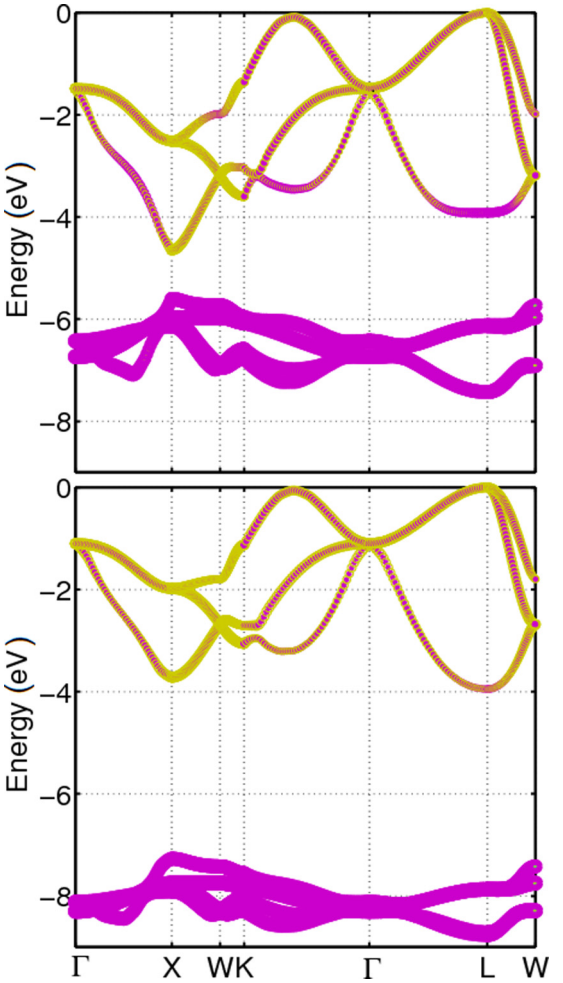

FIG. 2. Orbital character of CdO (RS) valence bands: (top) LDA and (bottom) LDA+A-$1/2$. The p character is represented in yellow and the d character in magenta.

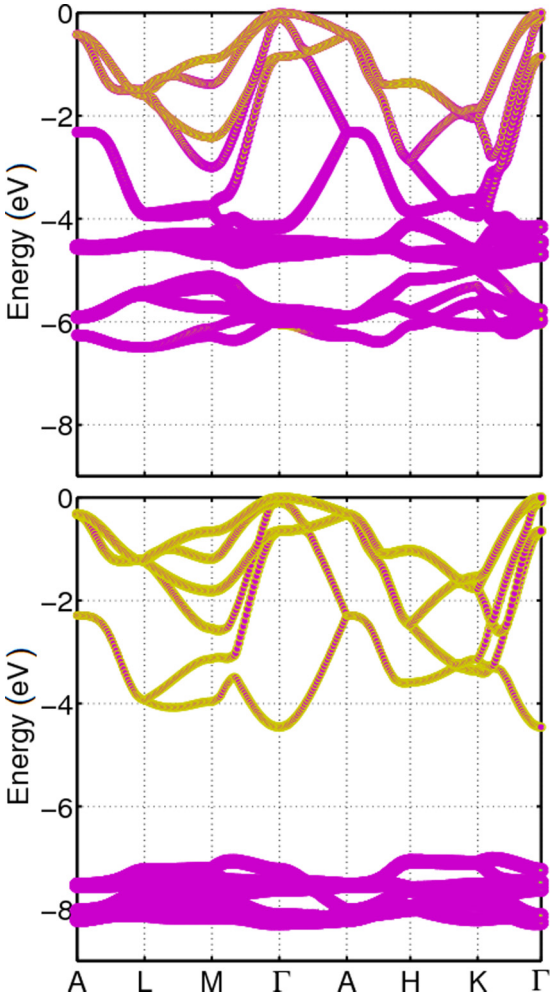

FIG. 3. Orbital character of ZnO (WZ) valence: (top) LDA and (bottom) LDA+A-1/2. The p character is represented in yellow and the d character in magenta.

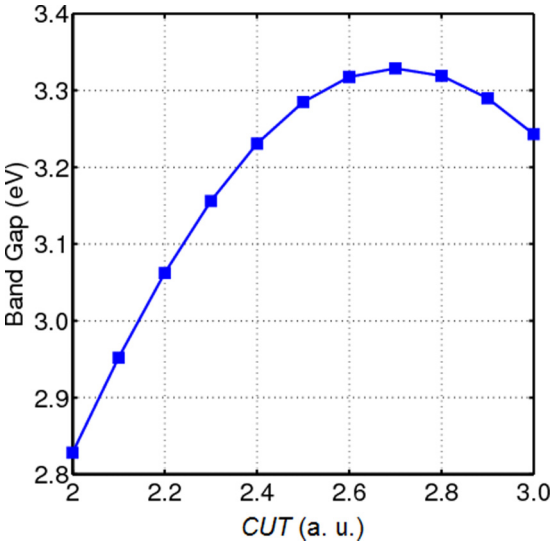

FIG. 4. Band gap vs CUT radius for (WZ) ZnO. The correction of the potential was obtained after the correction of cation Zn d orbital by LDA+A-1/2 framework.

TABLE II. CUT and A parameters utilized in the LDA-1/2 and LDA+A-1/2 quasiparticle corrections.

				CUT	
Method	Oxide	Structure	A	Cation	Anion
LDA+A-1/2	ZnO	WZ	1.57	1.48	2.70
		RS	1.71	1.48	2.60
		ZB	1.57	1.48	2.70
	CdO	WZ	1.06	2.56	2.90
		RS	1.11	2.56	2.70
		ZB	1.04	2.56	2.90
LDA-1/2	MgO	WZ	1.00		2.80
		RS	1.00		2.60
		ZB	1.00		2.80

leading to strong pd interactions with the $2p$ oxygen bands, at least in fourfold coordinated systems but not in rocksalt geometries [51], in disagreement with the experimental data. For instance, the d semicore position in WZ ZnO is about 7.3–8.8 eV [14–21], while in DFT GGA calculation it records 5.0 eV [11]. This underestimation increases the d character of the VBM and shrinks the energy gap in addition to standard DFT underestimation. Direct application of LDA-1/2 on ZnO, only considering 1/2 electron in O p or sharing 1/2 electron between O p and Zn d according to the character of the VBM, leads to an improvement but still much smaller gaps compared to experimental values. A good band gap (3.2 eV) can be obtained when the 1/2 electron is removed from both O p and Zn d. This procedure has been described in the original LDA-1/2 paper [42]. Despite the fact that one obtains a good value for the gap, the position of d band is even worse than in standard DFT. In this context, it is clear that in the case of CdO and ZnO, an entirely improved band structure can be obtained dealing not only with the energy gap regions, as in the original implementation of LDA-1/2, but also in some way solving the problem of d band localization.

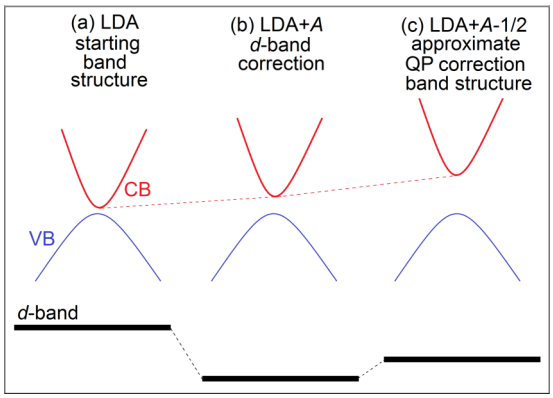

FIG. 5. Schematic representation of conduction band (CB) in red, valence band (VB) in blue, and d bands in black for ZnO and CdO. The reference energy for the three cases is taken as VBM. The case (a) indicates the LDA calculation, (b) the correction of d band by increase of amplitude A, and (c) the complete correction, with the application of standard LDA-1/2 method.

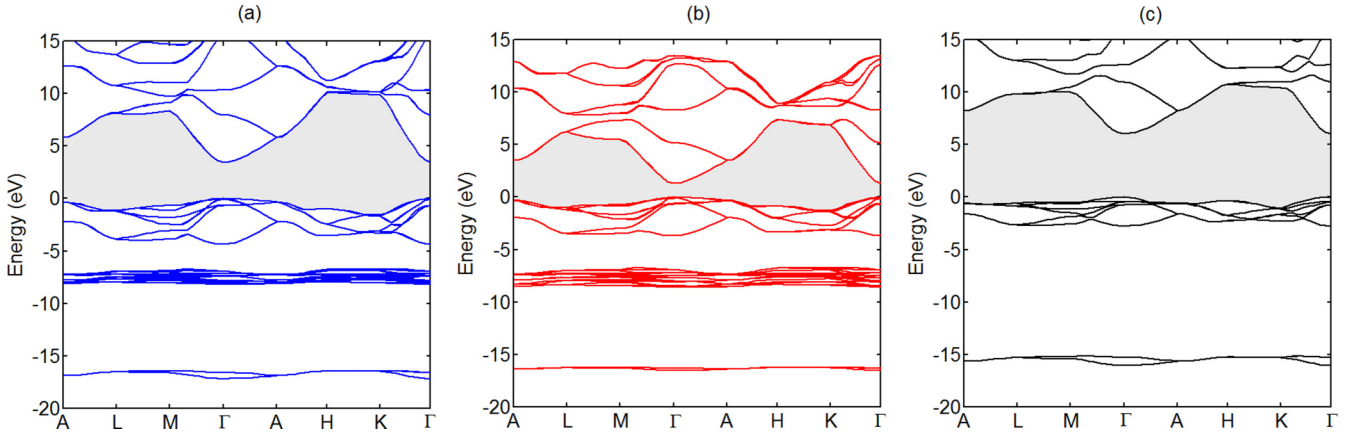

FIG. 6. Band structures within LDA+A-1/2 approach for the WZ phase of (a) ZnO and (b) CdO and LDA-1/2 approach (c) for MgO. The spin orbit (SO) and crystal field (CF) parameters are calculated using the quasicubic model for ZnO and CdO. (a) ZnO: $\Delta_{CF} = 35.1$ meV and $\Delta_{SO} = -0.7$ meV, (b) CdO: $\Delta_{CF} = 53.8$ meV and $\Delta_{SO} = -33.1$ meV, and (c) MgO: $\Delta_{SO} = 23.1$ meV.

C. Generalization

The LDA-1/2 approach is based on the assumption that the self-energy potential obtained from an atomic calculation is reasonable to provide the right correction in the case of an infinite solid. It usually works very well for the majority of cases of semiconductors, adding the right amount of correction needed for the VBM states in order to obtain energy gaps comparable with experimental values. However, this approximation is not so efficient for much more localized states, such as the shallow cation d bands in ZnO and CdO.

The improvement of the LDA-1/2 method starts with the idea to get an improved d-band position before the application of the standard LDA-1/2 method. This can be implemented within the LDA-1/2 method in the following way. The potential V_S in equation (1) is trimmed by a step function that depends mainly on two parameters, CUT, which defines the range of the correction, and the amplitude A. Usually in a LDA-1/2 calculation the amplitude A is set equal to 1 and the trimming of the self-energy potential (value of CUT) is determined variationally by making the fundamental band gap an extreme [42]. Here, we propose to use V_S in a first step to correct artificially the d band position provided by standard DFT by varying the A parameter. It is verified for a V_S potential generated by the subtraction of 1/2 electron of the d cation so that the increase of the A parameter is directly correlated with the linear increase of the binding energy of the cation d band. Figure 1 exemplifies this behavior for ZnO. Therefore, using the A variation we correct the position of the d band, E_d, based on the respective experimental values provided by the literature [14–21]. The increase of the amplitude A of the V_S potential shown in equation (1) indirectly decreases the pd hybridization, opening a little bit the energy gap.

For the corrections of the localized d bands, the CUT parameters come from a previous work [54], in which it is shown that they follow a linear relation with the atomic charge radius, keeping strongly their atomic character even in the solid. Using this relation, we obtain the values of $CUT = 1.48$ a.u. for Zn and 2.56 a.u. for Cd. The increased A parameter and the optimized Zn and Cd CUT radii provide an initially improved band structure for CdO and also ZnO. Table I indicates the character of the VBM before (LDA) and after this initial correction (LDA+A). The d band character of

TABLE III. The direct band gap $E_g(\Gamma_C - \Gamma_V)$. The width of the uppermost p-like valence band W_p and the average d band position below VBM E_d. All results are for WZ phase and the values are in eV. The theoretical results are divided into hybrid + GW (square brackets), others recipes of GW (brace), hybrid DFT (parentheses), and other DFT results.

Oxide	$E_g(\Gamma - \Gamma)$	W_p	E_d	Reference
	3.49	**4.35**	**7.45**	This Work
ZnO	0.73[a], (2.1[c]), {2.99[f]}, [3.2[b]] [3.2[c]], [3.21[d]], [3.37[f]], [3.6[e]]	3.99[g], 5.2[g], {4.9[e]}	5.0[a], [7.1[c]], [6.96[b]] [6.9[h]], [6.9[i]], [6.8[e]]	Theo.
	3.30[n], 3.37[m], 3.435[k] 3.436[j], 3.437[p], 3.438[o] 3.445[l], 3.53[q], 3.555[r]	5.3[g]	8.81[w], 8.5[v], 7.6[s], 7.5[t] 7.5[u], 7.4[c], 7.3[h], 6.95[x]	Exp.
CdO	**1.30**	**3.67**	**7.67**	This Work
	−0.34[ab], 0.9[aa], [0.96[x]], [1.06[z]]			Theo.
MgO	**6.06**	**2.75**		This Work
	3.78[ac], [6.19[y]], [6.52[z]]			Theo.

[a]Ref. [11]; [b]Ref. [41]; [c]Ref. [20]; [d]Ref. [36]; [e]Ref. [31]; [f]Ref. [32]; [g]Ref. [55]; [h]Ref. [21]; [i]Ref. [67]; [j]Ref. [68]; [k]Ref. [69]; [l]Ref. [70]; [m]Ref. [71]; [n]Ref. [72]; [o]Ref. [73]; [p]Ref. [74]; [q]Ref. [75]; [r]Ref. [76]; [s]Ref. [14]; [t]Ref. [15]; [u]Ref. [16]; [v]Ref. [17]; [w]Ref. [18]; [x]Ref. [19]; [y]Ref. [10]; [z]Ref. [56]; [aa]Ref. [77]; [ab]Ref. [62]; [ac]Ref. [78].

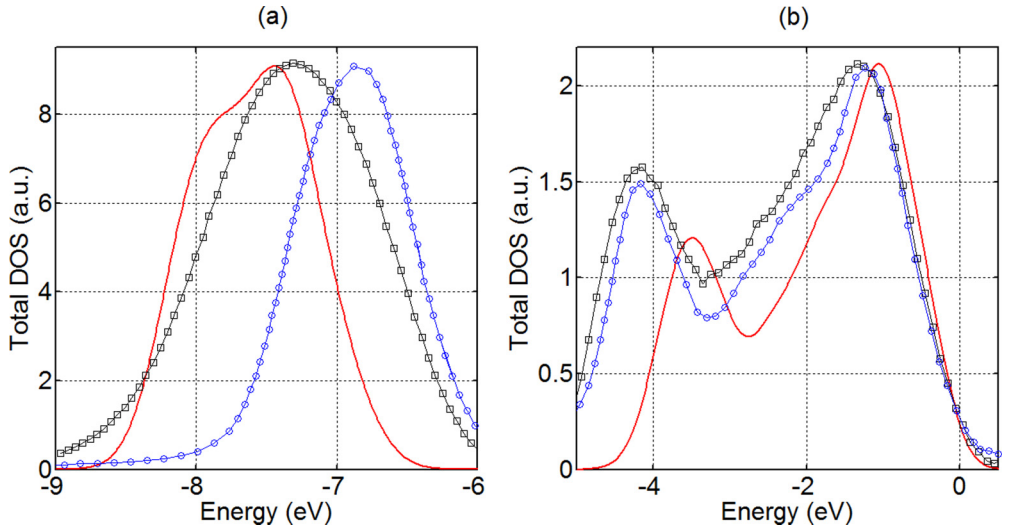

FIG. 7. Comparison between the LDA+A-1/2 total DOS (red), the G_0W_0@HSE03 DOS (blue), and XPS measurements (black) for WZ ZnO plotted in the range of (a) Zn3d bands and (b) O2p valence bands. Expt. data and G_0W_0@HSE03 DOS extracted from Ref. [21]. The VBM is used as energy zero.

the VBM decreases to about half of its initial value as the d band position is corrected in the case of ZnO. In the case of CdO the d character of the VBM decreases by about 40%. In Figs. 2 and 3 we present the resulting valence band structures, in LDA and LDA+A-1/2 approximation, including atomic orbital character, for ZnO and CdO. For both oxides the d band position moves toward a deeper position decreasing at the same time the amount of d character in the VBM. The pd hybridization is reduced resulting in a clear separation of O2p-derived uppermost valence bands and Zn3d–or Cd4d–derived lower semicore bands. As a consequence both bands are narrowed and the fundamental gaps opened (not shown in Figs. 2 and 3).

In the second step we improve the initial band structures employing the standard LDA-1/2 methodology. The character of VBM obtained from the improved band structure is then used to generate the fractions f related to the cation d and O p orbitals of the subtracted half electron. The CUT parameter for the O atom is obtained by maximizing the energy gap as usual. This procedure is exemplified in Fig. 4 for ZnO. We call this new method LDA+A-1/2.

For compounds that have structures different the most stable polymorphs named as ground state (GS) and the less energetically favorable polymorphs named as nonground state (NGS), e.g., RS and ZB for ZnO, and WZ and ZB for CdO, for which no experimental d band position is available, we consider the following procedure to obtain an estimated d band position for quasiparticle correction. Assuming that Δ_{LDA} is the difference $E_d^{NGS} - E_d^{GS}$ obtained through the LDA calculations, we assume that $E_d = E_d^{EXP} + \Delta_{LDA}$, where E_d^{EXP} is the experimental position of the d band for the GS structure. For NGS structures, we choose the A in order to obtain $E_d = E_d^{EXP} + \Delta_{LDA}$. In other words, we add the difference of the Kohn-Sham eigenvalues of the d levels in different crystallographic structures to the experimental binding energy in the equilibrium crystal structure to predict the d band positions in the nonequilibrium polymorphs.

In Table II all parameters utilized to perform LDA+A-1/2 and LDA-1/2 corrections are presented. The amplitude A obtained for the correct position of d band depends fundamentally on the compound, but is similar for zincblende and wurtzite structures with fourfold coordinated atoms. It deviates for the rocksalt geometry with a sixfold coordination. The CUT parameter for the oxygen atom is basically the same independent of the compound. The anion CUT parameter slightly depends on the polymorphic structure. Thus, the parameters can be considered as highly transferable. Only the amplitude A and the oxygen CUT have to be slightly modified, when changing the coordination of the atoms. A summary of the LDA+A-1/2 methodology, in particular the underlying three-step procedure, is illustrated in Fig. 5.

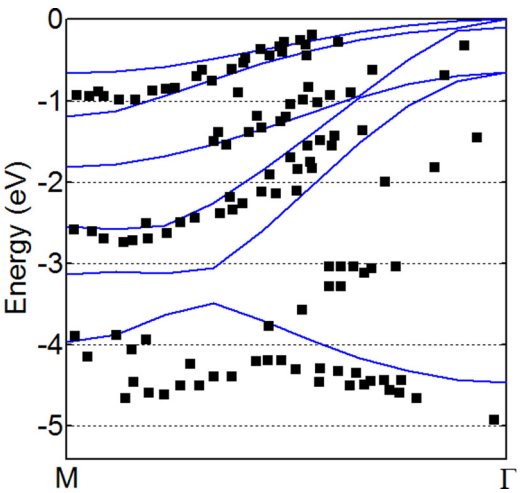

FIG. 8. Comparison between the ZnO (WZ) LDA+A-1/2 band structure (blue) and ARPES measurements (black squares). Expt. data extracted from Ref. [55].

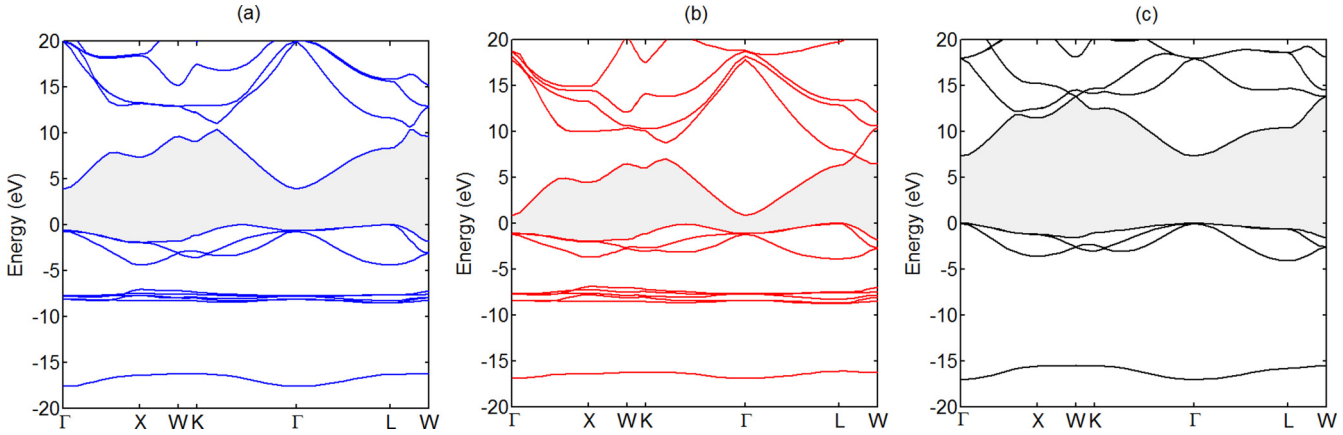

FIG. 9. Band structures within LDA+A-1/2 approach with SOC for RS (a) ZnO: $\Delta_{SO} = 48.0$ meV, (b) CdO: $\Delta_{SO} = 68.0$ meV, and LDA-1/2 approach (c) for MgO: $\Delta_{SO} = 37.8$ meV.

III. RESULTS AND DISCUSSIONS

A. Wurtzite

The final LDA+A-1/2 band structures for wurtzite ZnO, CdO, and MgO are displayed in Fig. 6. All three materials possess direct $\Gamma - \Gamma$ gaps; ZnO and CdO present similar band structures: an s band in the bottom, followed by localized d bands and a direct energy gap. The WZ MgO band structure shows a larger direct band gap because of the absence of d-semicore states, larger bond ionizities, and, in particular, the lighter cation. In Table III we summarize the results obtained for monoxides crystallizing in WZ structure. The

TABLE IV. The direct and indirect band gaps $E_g(\Gamma_C - \Gamma_V)$, $E_g(\Gamma_C - L_V)$. The width of the uppermost p-like valence band W_p and the average d band position below VBM E_d. All results are for RS phase and are in eV. The theoretical results are divided into hybrid + GW (square brackets), others recipes of GW (brace), hybrid DFT (parentheses), and other DFT results.

Oxide	$E_g(\Gamma - \Gamma)$	$E_g(\Gamma - L)$	W_p	E_d	Reference
ZnO	**4.57**	**3.93**	**4.40**	**7.81**	This Work
	1.57[d], 1.97[e], 2.60[b], 2.62[k], 2.73[a], {4.28[j]} {4.74[l]}, 5.09[f], 6.54[g]	0.75[d], 1.1[b], 1.1[c] 1.29[a], 1.47[d], 2.88[h] 4.51[f], {4.51[l]}, 5.54[g]	8.08[g]	5.57[a]	Theo.
	4.5[c], 4.5[j]	2.45[c], 2.7[i]			Expt.
CdO	**2.01**	**0.90**	**4.40**	**7.86**	This Work
	0.66[e], 0.8[u], 1.47[aa] 1.8[w], [1.90[n]], 2.36[x] 2.4[v], [2.45[m]], {2.88[aa]}	−0.6[ac], −0.43[e], 0.13[aa] 0.4[u], [0.68[m]], 0.8[v], [0.81[n]], [1.07[p]], 1.18[x], 1.3[w] {1.68[aa]}, 1.7[ac], 2.0[ac]	3.3[e], 4.1[v], 7.5[u]	14.4[u], {9[aa]}, 9.0[ac] [8.4[n]], [8.3[p]], 8.2[ac] 7[aa], 6.2[ac], 4.4[x] 4.3[v], 3.7[w]	Theo.
	1.2[aa], 2.0[aa], 2.16[ad], 2.28[s] 2.28[af], 2.4[r], 2.42[q]	0.55[t], 0.8[ac], 0.84[af], 0.9[r] 1.09[s], 1.09[ab], 1.2[z], 2.2[aa]		12.0[y], 12.0[ac], 10.7[ab] 9.4[ae], 8.8[p], 8.8[aa], 8.6[o]	Expt.
MgO	**7.35**		**4.06**		This Work
	4.34[aj], 4.5[e], 4.56[aj], 4.63[am] 4.7[ai], 4.76[ah], 4.76[ak], 4.79[am] 4.86[am], 4.92[aj], 4.93[am], 5.24[ag] (6.44[am]), [6.22[ah]], (6.50[aj]), (6.67[am]) (7.04[am]), (7.07[am]), 7.17[ai], (7.18[am]) {7.25[ah]}, {7.25[ak]}, (7.35[am]), [7.47[an]] [7.49[m]], [7.49[h]], {7.72[ak]}, {7.88[am]}, (7.94[ah]), {8.12[al]} {8.25[al]}, {8.47[ak]}, {9.16[al]}				Theo.
	7.22[aj], 7.7[e], 7.77[an] 7.77[ao], 7.83[ap]				Expt.

[a]Ref. [79]; [b]Ref. [80]; [c]Ref. [58]; [d]Ref. [81]; [e]Ref. [11]; [f]Ref. [82]; [g]Ref. [83]; [h]Ref. [10]; [i]Ref. [61]; [j]Ref. [60]; [k]Ref. [62]; [l]Ref. [84]; [m]Ref. [36]; [n]Ref. [41]; [o]Ref. [52]; [p]Ref. [21]; [q]Ref. [85]; [r]Ref. [86]; [s]Ref. [59]; [t]Ref. [87]; [u]Ref. [88]; [v]Ref. [89]; [w]Ref. [90]; [x]Ref. [91]; [y]Ref. [14]; [z]Ref. [92]; [aa]Ref. [53]; [ab]Ref. [93]; [ac]Ref. [94]; [ad]Ref. [95]; [ae]Ref. [96]; [af]Ref. [9]; [ag]Ref. [78]; [ah]Ref. [97]; [ai]Ref. [98]; [aj]Ref. [99]; [ak]Ref. [38]; [al]Ref. [100]; [am]Ref. [101]; [an]Ref. [102]; [ao]Ref. [103]; [ap]Ref. [104].

energy gap obtained for ZnO is 3.49 eV in good agreement with experimental results. Subtracting the exciton binding energy the difference is less than 0.1 eV. Recent GW-related results present a variation of about 0.5 eV below the experimental ones. All the results point out that LDA+A-1/2 calculations are comparable with the best GW results with a computing time much lower than GW and/or hybrid calculations. The situation is similar for the two other oxides, CdO and MgO.

The density of states below the valence band maximum is displayed in Fig. 7. As in Ref. [21], it presents the Shirley-background-subtracted valence-band x-ray photoemission spectroscopy (XPS) measurements around the Zn3d levels (a) and the topmost valence band (b) of WZ ZnO, along with the calculated G_0W_0@HSE03 DOS without lifetime and instrumental broadening. Additionally, we plot the Gaussian broadened LDA+A-1/2 total DOS. In Fig. 7(b), we can see that the topmost valence band region presents a two-peak structure, as observed from valence band XPS measurements [21]. In order to realize the comparison with LDA+A-1/2 total DOS we adjust the main peaks to present the same DOS amplitude of experimental result. A good agreement is obtained between our calculation and experiment, indicating that the LDA+A-1/2 calculations reasonably correct the Zn3d position. For the valence band, there is a qualitative agreement in terms of the lineshape with double-peak structure. However, the peaks are too close to the VBM, and the bandwidth in LDA+A-1/2 is narrow compared to the measurements. In terms of relative intensity of the peaks, there is, however, a good concordance between experiment and theory.

Additionally, Fig. 8 depicts the comparison between the ZnO (WZ) LDA+A-1/2 and ARPES data [55] along the $M-\Gamma$ high-symmetry line in the BZ in the oxygen 2p orbital region. One observes a good accordance between experimental data and the higher oxygen 2p bands. As mentioned above, the LDA+A-1/2 O2p correction makes the width of valence band to be narrower compared to the measured one. However, a rigid shift of the fifth valence band by about 1 eV and the sixth one by 0.4 eV brings also the lower O2p valence bands close to the measured ones.

The spin orbit Δ_{SO} and crystal field Δ_{CF} splittings are calculated using the quasicubic model for ZnO and CdO. We obtain a Δ_{CF} of 35.1 meV for ZnO and 53.8 meV for CdO. For Δ_{SO} we obtain -0.7 meV for ZnO, -33.1 meV for CdO, and 23.1 meV for MgO. The values are compatible with other theoretical results [56,57].

B. Rocksalt

Rocksalt is the most stable structure of CdO and MgO, even though for ZnO this polymorph can be obtained experimentally under high pressure conditions [58]. The final LDA+A-1/2 band structures of RS ZnO and RS CdO, in Figs. 9(a) and 9(b), are very similar. Both present an indirect energy gap between the VBM at the L point and the CBM at the Γ point. Additionally, a second maximum quite pronounced along the path $\Gamma-K$ and the CBM occurs at the Γ point. While the dispersion and position of the valence bands are close to each other, the lowest s-like conduction band and also the higher conduction bands are lower in energy for CdO because of the lower ionicity of the related Cd-O bonds and heavier atom Cd. In contrast, MgO, whose band structure is depicted in Fig. 8 (c), has a direct $\Gamma-\Gamma$ band gap.

Table IV presents the characteristic energies for RS ZnO, RS CdO, and RS MgO. For RS CdO we calculate a direct gap of 2.01 eV that agrees well with the result of 2.28 eV [59]. The indirect fundamental band gap is 0.90 eV very close to the most experimental results presented in Table IV which range from 0.8 to 1.2 eV. Here the GW results are dispersed as well, ranging from 0.68 eV [36] to 1.68 [53]. The width of the topmost valence band is 4.40 eV and the Cd4d band position is -7.86 eV. That is a good result even being more shallow than the results of other quasiparticle methods and experimental data. For RS ZnO we obtain a direct gap of 4.57 eV that agrees with the value of 4.5 eV found experimentally [58,60]. The RS ZnO indirect gap of 3.93 eV is larger than the experimental value [58,61]. For CdO and MgO there are no experimental data for comparison with our result for W_p. For RS MgO the direct band gap is 7.35 eV and confirms that the LDA-1/2

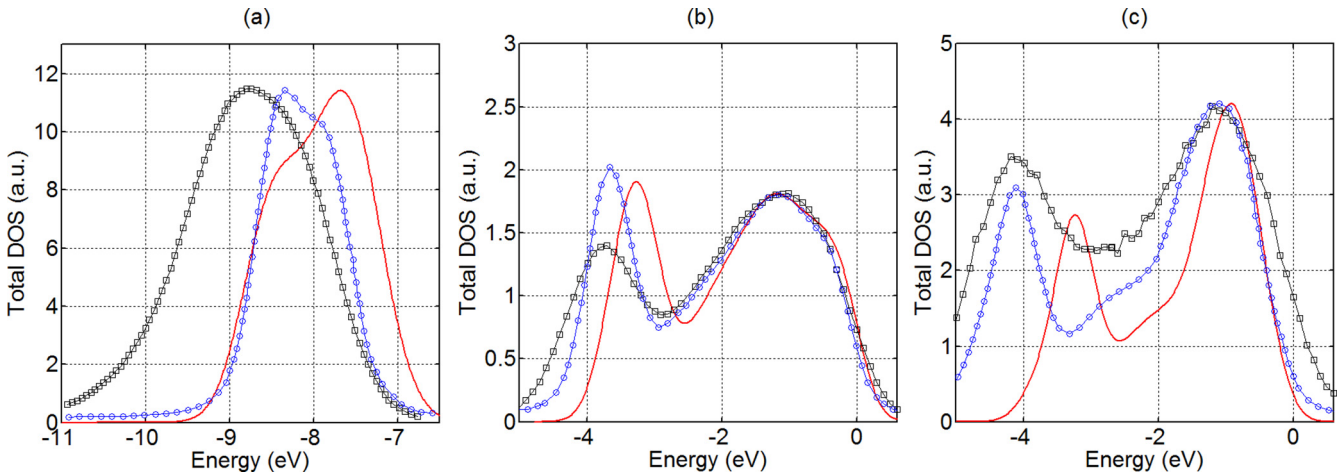

FIG. 10. Comparison between the LDA+A-1/2 total DOS (red), the G_0W_0@HSE03 DOS (blue), and XPS measurements (black) for RS CdO plotted in the range of (a) Cd4d bands, (b) O2p valence bands. (c) LDA-1/2 total DOS (red), the G_0W_0@HSE03 DOS (blue), and XPS measurements (black) for RS MgO in the range of O2p valence bands. Expt. data and G_0W_0@HSE03 DOS extracted from Ref. [21]. The VBM is used as energy zero.

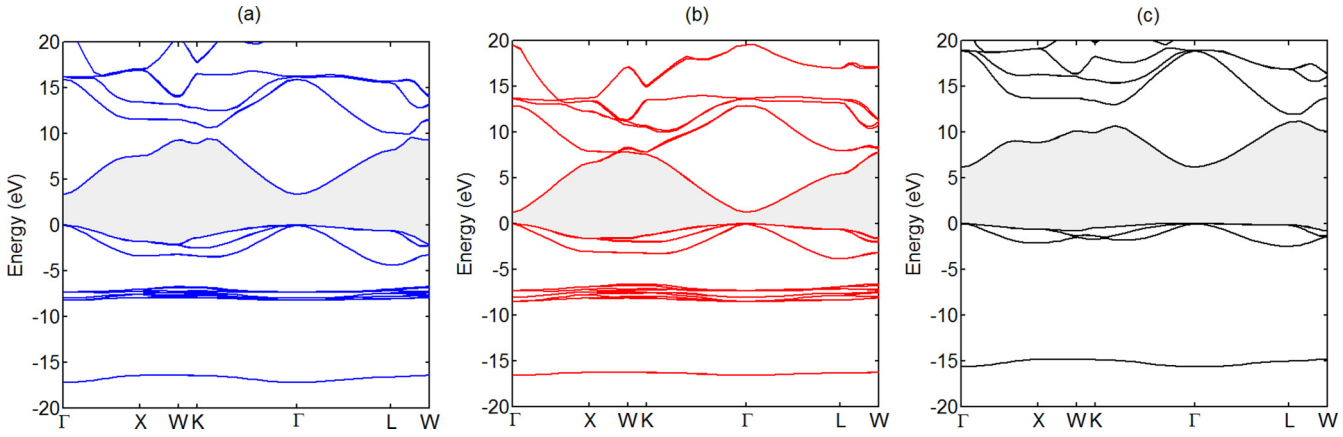

FIG. 11. Band structures within LDA+A-1/2 approach with SOC for ZB (a) ZnO: $\Delta_{SO} = 2.1$ meV, (b) CdO: $\Delta_{SO} = -28.1$ meV, and LDA-1/2 approach (c) for MgO: $\Delta_{SO} = 34.0$ meV.

method gives a good result for gaps of compounds without semicore states. Another interesting point is the spin-orbit splitting of the three uppermost valence bands at Γ. There is a change in sign from WZ to RS, at least for ZnO and CdO, and a general increase, e.g., in the MgO case from 23.1 to 37.8 meV. The reasons have been discussed elsewhere [57]. The Δ_{SO} is 48.0 meV for ZnO and 68.0 meV for CdO. The values are compatible with other theoretical results [56,62].

The density of occupied states is displayed in Fig. 10 together with the LDA+A-1/2 total DOS (RS CdO); we also show the LDA-1/2 total DOS (RS MgO). In Fig. 10(a), which displays Cd4d spectra, we state a qualitatively agreement between the LDA+A-1/2 DOS, the G_0W_0@HSE03 DOS, and XPS measurements. In the Cd4d region, both the G_0W_0@HSE03 DOS and LDA+A-1/2 DOS show a double peak structure in contrast to XPS that is more pronounced in the LDA+A-1/2 DOS. However, the peak position and, therefore, the theoretical binding energy is somewhat underestimated compared to XPS measurements. In the topmost valence band region for CdO in Fig. 10(b), the accordance between G_0W_0@HSE03 DOS and LDA+A-1/2 DOS is reasonable. In both approximations two peaks are almost coincident. The low-energy peak of LDA+A-1/2 DOS is somewhat higher in energy than the corresponding peak in the G_0W_0@HSE03 DOS plot. The quasiparticle DOS peak around −4 eV agrees better with the XPS measurements than the results of the LDA+A-1/2 method.

Figure 10(c) depicts the XPS measurements, the broadened G_0W_0@HSE03 DOS, and the LDA-1/2 DOS for the topmost valence band region of RS MgO. Qualitatively, concerning the lineshape with a double-peak structure, the quasiparticle plots are very similar. The difference again is that the LDA-1/2 DOS is narrower than the G_0W_0@HSE03 DOS. This observation is explained by the fact that LDA-1/2 localizes the bands to which the correction was applied, here to the oxygen p orbitals.

C. Zincblende

The zincblende structure is not the most stable polymorph for one of the oxides ZnO, CdO, and MgO, but it is for many other important compound semiconductors such as the arsenides and the phosphides. Under certain conditions, ZB ZnO can be grown on a GaAs(001) substrate [63,64]. Therefore, we study this polymorph for completeness and predict its electronic properties.

For all three cations Zn, Cd, and Mg, the ZB polymorph presents a direct gap at Γ as shown in Fig. 11. Again, the band

TABLE V. The direct band gap $E_g(\Gamma_C - \Gamma_V)$. The width of the uppermost valence band, W_p and the average d band position below VBM E_d. All results are for ZB phase and are in eV. The theoretical results are divided into GW (brace) and others DFT results.

Oxide	$E_g(\Gamma-\Gamma)$	W_p	E_d	Reference
	3.37	**4.39**	**7.50**	This Work
	0.2[b], 0.75[b], 1.1[b], 2.26[a]		8.9[b], 8.66[b], 7.8[b], 7.5[b]	Theo.
ZnO	3.5[b], 3.50[a], {3.6[b]}		{6.6[b]}, 5.4[b], 5.3[b], 5.0[b]	
	3.75[b], 3.8[b], 11.70[a]			
	3.12[h], 3.22[h], 3.26[i], 3.27[d]			Exp.
	3.27[e], 3.27[f], 3.28[g], 3.368[c]			
CdO	**1.22**	**3.84**	**7.57**	This Work
	−0.42[j], 0.0[k]			Theo.
MgO	**6.20**	**2.47**		This Work
	3.5[k], 3.59[j]			Theo.

[a]Ref. [105]; [b]Ref. [65]; [c]Ref. [106]; [d]Ref. [63]; [e]Ref. [107]; [f]Ref. [64]; [g]Ref. [108]; [h]Ref. [109]; [i]Ref. [110]; [j]Ref. [62]; [k]Ref. [11].

structures for ZB ZnO and ZB CdO are similar with gaps of 3.37 eV of ZnO and 1.22 eV of CdO. The average Zn3*d* band position is −7.50 eV below the VBM and −7.57 eV for the Cd4*d* band position. The result for the Zn3*d* band position is in good agreement with other calculations [65]. In both cases the ZB gaps are approximately 0.1 eV smaller than WZ gaps as for the nitrides AlN, GaN, and InN [66]. However, for MgO, the WZ gap is 0.14 eV larger than the ZB gap.

Table V presents the results for the direct band gap at Γ point, the width of the topmost valence band, and the average *d*-band position in comparison with experimental and theoretical results for ZB ZnO. For ZB CdO and ZB MgO the comparison is made with other calculations. We also obtain very good agreement between our calculations and experiments for the energy gap of ZB ZnO. Apart from the folding of the larger BZ (ZB) to the smaller one (WZ), the bands also exhibit similarities comparing Fig. 6 with Fig. 11. Even the spin-orbit splittings of the uppermost valence bands, Δ_{SO}, are close to each other.

IV. SUMMARY AND CONCLUSIONS

In this work we developed a low computational cost method for electronic structure calculations on the quasiparticle level for nonmetals that possess shallow core levels. It has been applied to the band structure of the monoxides ZnO, CdO, and MgO in three different polymorphic WZ, RS, and ZB structures. The improved approach is achieved by introducing in the LDA-1/2 method an amplitude factor A which is responsible for placing the *d* bands at the experimental binding energy. This new methodology is named as LDA+A-1/2, accordingly.

ZnO and CdO present a direct gap in WZ and ZB structures but an indirect gap in RS structure. The fundamental gaps do not change very much considering these two polymorphs. However, MgO is always a direct gap material with low band dispersion. In general, the electronic properties of WZ and ZB are very similar for all compounds. The energy gap is about 1.0 eV higher in RS compared with WZ and ZB. Comparing the energy gap and the *d* band position directly with experiments we demonstrated the good quality of the new computational quasiparticle scheme. Additionally, the comparison with other theoretical approaches including quasiparticle corrections shows at least the same level of accuracy, verifying the good reliability of the method, despite its simplicity in the implementation and low computational cost. We also have obtained reasonable agreement in the comparison with valence band x-ray photoemission spectroscopy, at least for the lineshape and the peak close to the valence band maximum. The Δ_{SO} is 2.1 meV for ZnO, −28.1 meV for CdO, and 34.0 meV for MgO.

These results show the potential of the LDA+A-1/2 method for ZnO and CdO and for complex systems composed by these oxides, like heterojunctions and alloys, where GW on top of the hybrid functionals is prohibited for computational costs. The method used for *d* semicore states can also be easily applied to *shallow f* electron bands. Some additional advantages are that the methodology can also be applied to include gradient contributions in the XC potential and also SO interaction.

ACKNOWLEDGMENT

This work was supported by the Brazilian funding agency CNPq [Grants. No. 311060/2013-7 and No. 305405/2014-4].

[1] S. Nakamura, S. Pearton, and G. Fasol, *The Blue Laser Diode: The Complete Story* (Springer, Berlin, Heidelberg, 2013).
[2] D. M. Bagnall, Y. F. Chen, Z. Zhu, T. Yao, S. Koyama, M. Y. Shen, and T. Goto, Appl. Phys. Lett. **70**, 2230 (1997).
[3] A. Ghis, R. Meyer, P. Rambaud, F. Levy, and T. Leroux, IEEE Trans. Electron Devices **38**, 2320 (1991).
[4] B. Sang, A. Yamada, and M. Konagai, Jpn. J. Appl. Phys. **37**, L206 (1998).
[5] N. Dayan, S. Sainkar, R. Karekar, and R. Aiyer, Thin Solid Films **325**, 254 (1998).
[6] C. R. Gorla, N. W. Emanetoglu, S. Liang, W. E. Mayo, Y. Lu, M. Wraback, and H. Shen, J. Appl. Phys. **85**, 2595 (1999).
[7] Y. Chen, D. M. Bagnall, H.-j. Koh, K.-t. Park, K. Hiraga, Z. Zhu, and T. Yao, J. Appl. Phys. **84**, 3912 (1998).
[8] I. Vurgaftman, J. R. Meyer, and L. R. Ram-Mohan, J. Appl. Phys. **89**, 5815 (2001).
[9] I. Broser, R. Broser, H. Finkenrath, R. R. Galazka, H. E. Gumlich, A. Hoffmann, J. Kossut, E. Mollwo, H. Nelkowski, G. Nimtz, W. von der Osten, M. Rosenzweig, H. J. Schulz, D. Theis, and D. Tschierse, in *Physics of II-VI and I-VII Compounds, Semimagnetic Semiconductors*, edited by O. Madelung (Springer-Verlag, Berlin, Heidelberg, 1982), Vol. 17b.
[10] A. Schleife, C. Rödl, J. Furthmüller, and F. Bechstedt, New J. Phys. **13**, 085012 (2011).
[11] A. Schleife, F. Fuchs, J. Furthmüller, and F. Bechstedt, Phys. Rev. B **73**, 245212 (2006).
[12] D. M. Ceperley and B. J. Alder, Phys. Rev. Lett. **45**, 566 (1980).
[13] J. P. Perdew and Y. Wang, Phys. Rev. B **46**, 12947 (1992).
[14] C. J. Vesely and D. W. Langer, Phys. Rev. B **4**, 451 (1971).
[15] R. A. Powell, W. E. Spicer, and J. C. McMenamin, Phys. Rev. Lett. **27**, 97 (1971).
[16] R. A. Powell, W. E. Spicer, and J. C. McMenamin, Phys. Rev. B **6**, 3056 (1972).
[17] C. J. Vesely, R. L. Hengehold, and D. W. Langer, Phys. Rev. B **5**, 2296 (1972).
[18] L. Ley, R. A. Pollak, F. R. McFeely, S. P. Kowalczyk, and D. A. Shirley, Phys. Rev. B **9**, 600 (1974).
[19] R. Girard, O. Tjernberg, G. Chiaia, S. Söderholm, U. Karlsson, C. Wigren, H. Nylén, and I. Lindau, Surf. Sci. **373**, 409 (1997).
[20] A. R. H. Preston, B. J. Ruck, L. F. J. Piper, A. DeMasi, K. E. Smith, A. Schleife, F. Fuchs, F. Bechstedt, J. Chai, and S. M. Durbin, Phys. Rev. B **78**, 155114 (2008).
[21] P. D. C. King, T. D. Veal, A. Schleife, J. Zúñiga-Pérez, B. Martel, P. H. Jefferson, F. Fuchs, V. Muñoz-Sanjosé, F. Bechstedt, and C. F. McConville, Phys. Rev. B **79**, 205205 (2009).

[22] J. Heyd, G. E. Scuseria, and M. Ernzerhof, J. Chem. Phys. **118**, 8207 (2003).

[23] J. Heyd, G. E. Scuseria, and M. Ernzerhof, J. Chem. Phys. **124**, 219906 (2006).

[24] L. Hedin, Phys. Rev. **139**, A796 (1965).

[25] M. S. Hybertsen and S. G. Louie, Phys. Rev. Lett. **55**, 1418 (1985).

[26] M. S. Hybertsen and S. G. Louie, Phys. Rev. B **34**, 5390 (1986).

[27] F. Fuchs, J. Furthmüller, F. Bechstedt, M. Shishkin, and G. Kresse, Phys. Rev. B **76**, 115109 (2007).

[28] J. Wróbel, K. J. Kurzydłowski, K. Hummer, G. Kresse, and J. Piechota, Phys. Rev. B **80**, 155124 (2009).

[29] C. Di Valentin, S. Botti, and M. Cococcioni, *First Principles Approaches to Spectroscopic Properties of Complex Materials* (Springer, Berlin, 2014), Vol. 347.

[30] M. Usuda, N. Hamada, T. Kotani, and M. van Schilfgaarde, Phys. Rev. B **66**, 125101 (2002).

[31] B.-C. Shih, Y. Xue, P. Zhang, M. L. Cohen, and S. G. Louie, Phys. Rev. Lett. **105**, 146401 (2010).

[32] C. Friedrich, M. C. Müller, and S. Blügel, Phys. Rev. B **83**, 081101 (2011).

[33] M. Stankovski, G. Antonius, D. Waroquiers, A. Miglio, H. Dixit, K. Sankaran, M. Giantomassi, X. Gonze, M. Côté, and G.-M. Rignanese, Phys. Rev. B **84**, 241201 (2011).

[34] A. Schleife, C. Rödl, F. Fuchs, J. Furthmüller, and F. Bechstedt, Phys. Rev. B **80**, 035112 (2009).

[35] F. Bechstedt, *Many-Body Approach to Electronic Excitations* (Springer, Berlin, 2015), Vol. 181.

[36] A. Schleife, F. Fuchs, C. Rödl, J. Furthmüller, and F. Bechstedt, Appl. Phys. Lett. **94**, 012104 (2009).

[37] R. W. Godby, M. Schlüter, and L. J. Sham, Phys. Rev. B **37**, 10159 (1988).

[38] M. Shishkin and G. Kresse, Phys. Rev. B **75**, 235102 (2007).

[39] W. Chen and A. Pasquarello, Phys. Rev. B **86**, 035134 (2012).

[40] J. Klimeš, M. Kaltak, and G. Kresse, Phys. Rev. B **90**, 075125 (2014).

[41] A. Schleife, C. Rödl, F. Fuchs, J. Furthmüller, F. Bechstedt, P. Jefferson, T. D. Veal, C. F. McConville, L. Piper, A. DeMasi *et al.*, J. Korean Phys. Soc. **53**, 2811 (2008).

[42] L. G. Ferreira, M. Marques, and L. K. Teles, Phys. Rev. B **78**, 125116 (2008).

[43] P. E. Blöchl, Phys. Rev. B **50**, 17953 (1994).

[44] G. Kresse and J. Furthmüller, Phys. Rev. B **54**, 11169 (1996).

[45] H. J. Monkhorst and J. D. Pack, Phys. Rev. B **13**, 5188 (1976).

[46] D. Hobbs, G. Kresse, and J. Hafner, Phys. Rev. B **62**, 11556 (2000).

[47] L. G. Ferreira, M. Marques, and L. K. Teles, AIP Adv. **1**, 032119 (2011).

[48] J. C. Slater and K. H. Johnson, Phys. Rev. B **5**, 844 (1972).

[49] J. F. Janak, Phys. Rev. B **18**, 7165 (1978).

[50] R. R. Pelá, C. Caetano, M. Marques, L. G. Ferreira, J. Furthmüller, and L. K. Teles, Appl. Phys. Lett. **98**, 151907 (2011).

[51] S.-H. Wei and A. Zunger, Phys. Rev. B **37**, 8958 (1988).

[52] L. F. J. Piper, A. DeMasi, K. E. Smith, A. Schleife, F. Fuchs, F. Bechstedt, J. Zúñiga-Pérez, and V. Muñoz-Sanjosé, Phys. Rev. B **77**, 125204 (2008).

[53] H. Dixit, D. Lamoen, and B. Partoens, J. Phys.: Condens. Matter **25**, 035501 (2013).

[54] R. R. Pelá, M. Marques, L. G. Ferreira, J. Furthmüller, and L. K. Teles, Appl. Phys. Lett. **100**, 202408 (2012).

[55] H. Morkoç and Ü. Özgür, *Zinc Oxide: Fundamentals, Materials and Device Technology* (John Wiley & Sons, Berlin, 2008).

[56] A. Schleife, F. Fuchs, C. Rödl, J. Furthmüller, and F. Bechstedt, Phys. Status Solidi B **246**, 2150 (2009).

[57] A. Schleife, C. Rödl, F. Fuchs, J. Furthmüller, and F. Bechstedt, Appl. Phys. Lett. **91**, 241915 (2007).

[58] A. Segura, J. A. Sans, F. J. Manjón, A. Muñoz, and M. J. Herrera-Cabrera, Appl. Phys. Lett. **83**, 278 (2003).

[59] F. P. Koffyberg, Phys. Rev. B **13**, 4470 (1976).

[60] H. Dixit, R. Saniz, D. Lamoen, and B. Partoens, Comput. Phys. Commun. **182**, 2029 (2011).

[61] P. A. Rodnyi and I. V. Khodyuk, Opt. Spectrosc. **111**, 776 (2011).

[62] Y. Z. Zhu, G. D. Chen, H. Ye, A. Walsh, C. Y. Moon, and S.-H. Wei, Phys. Rev. B **77**, 245209 (2008).

[63] A. B. M. A. Ashrafi, A. Ueta, A. Avramescu, H. Kumano, I. Suemune, Y.-W. Ok, and T.-Y. Seong, Appl. Phys. Lett. **76**, 550 (2000).

[64] A. Ashrafi, A. Ueta, H. Kumano, and I. Suemune, J. Cryst. Growth **221**, 435 (2000).

[65] A. Qteish, J. Phys.: Condens. Matter **12**, 5639 (2000).

[66] L. C. de Carvalho, A. Schleife, and F. Bechstedt, Phys. Rev. B **84**, 195105 (2011).

[67] S.-H. Jang and S. F. Chichibu, J. Appl. Phys. **112**, 073503 (2012).

[68] D. Thomas, J. Phys. Chem. Solids **15**, 86 (1960).

[69] Y. S. Park, C. W. Litton, T. C. Collins, and D. C. Reynolds, Phys. Rev. **143**, 512 (1966).

[70] W. Y. Liang and A. D. Yoffe, Phys. Rev. Lett. **20**, 59 (1968).

[71] A. Mang, K. Reimann, and S. Rübenacke, Solid State Commun. **94**, 251 (1995).

[72] V. Srikant and D. R. Clarke, J. Appl. Phys. **83**, 5447 (1998).

[73] K. Thonke, T. Gruber, N. Teofilov, R. Schönfelder, A. Waag, and R. Sauer, Phys. B: Condens. Matter **308–310**, 945 (2001).

[74] A. Teke, Ü. Özgür, S. Doğan, X. Gu, H. Morkoç, B. Nemeth, J. Nause, and H. O. Everitt, Phys. Rev. B **70**, 195207 (2004).

[75] S. Tsoi, X. Lu, A. K. Ramdas, H. Alawadhi, M. Grimsditch, M. Cardona, and R. Lauck, Phys. Rev. B **74**, 165203 (2006).

[76] H. Alawadhi, S. Tsoi, X. Lu, A. K. Ramdas, M. Grimsditch, M. Cardona, and R. Lauck, Phys. Rev. B **75**, 205207 (2007).

[77] A. Janotti and C. G. Van de Walle, Phys. Rev. B **75**, 121201 (2007).

[78] S. Limpijumnong and W. R. L. Lambrecht, Phys. Rev. B **63**, 104103 (2001).

[79] J. Sun, H.-T. Wang, J. He, and Y. Tian, Phys. Rev. B **71**, 125132 (2005).

[80] B. Amrani, I. Chiboub, S. Hiadsi, T. Benmessabih, and N. Hamdadou, Solid State Commun. **137**, 395 (2006).

[81] Z. Charifi, H. Baaziz, and A. Hussain Reshak, Phys. Status Solidi B **244**, 3154 (2007).

[82] D. Fritsch, H. Schmidt, and M. Grundmann, Appl. Phys. Lett. **88**, 134104 (2006).

[83] J. E. Jaffe, R. Pandey, and A. B. Kunz, Phys. Rev. B **43**, 14030 (1991).

[84] H. Q. Ni, Y. F. Lu, and Z. M. Ren, J. Appl. Phys. **91**, 1339 (2002).

[85] C. Sravani, K. R. Reddy, and P. Reddy, Mater. Lett. **15**, 356 (1993).
[86] I. Demchenko, M. Chernyshova, T. Tyliszczak, J. Denlinger, K. Yu, D. Speaks, O. Hemmers, W. Walukiewicz, G. Derkachov, and K. Lawniczak-Jablonska, J. Electron Spectrosc. Relat. Phenom. **184**, 249 (2011).
[87] H. Köhler, Solid State Commun. **11**, 1687 (1972).
[88] J. C. Boettger and A. B. Kunz, Phys. Rev. B **27**, 1359 (1983).
[89] K. Maschke and U. Rössler, Phys. Status Solidi B **28**, 577 (1968).
[90] S. Tewari, Solid State Commun. **12**, 437 (1973).
[91] A. Breeze and P. Perkins, Solid State Commun. **13**, 1031 (1973).
[92] C. McGuinness, C. B. Stagarescu, P. J. Ryan, J. E. Downes, D. Fu, K. E. Smith, and R. G. Egdell, Phys. Rev. B **68**, 165104 (2003).
[93] L. Piper, P. Jefferson, T. Veal, C. McConville, J. Zúñiga-Pérez, and V. Muñoz-Sanjosé, Superlattices Microstruct. **42**, 197 (2007).
[94] D. Vogel, P. Krüger, and J. Pollmann, Phys. Rev. B **54**, 5495 (1996).
[95] P. H. Jefferson, S. A. Hatfield, T. D. Veal, P. D. C. King, C. F. McConville, J. Zúñiga-Pérez, and V. Muñoz-Sanjosé, Appl. Phys. Lett. **92**, 022101 (2008).
[96] Y. Dou, R. G. Egdell, D. S. L. Law, N. M. Harrison, and B. G. Searle, J. Phys.: Condens. Matter **10**, 8447 (1998).
[97] F. Bechstedt, F. Fuchs, and G. Kresse, Phys. Status Solidi B **246**, 1877 (2009).
[98] F. Tran and P. Blaha, Phys. Rev. Lett. **102**, 226401 (2009).
[99] J. Heyd, J. E. Peralta, G. E. Scuseria, and R. L. Martin, J. Chem. Phys. **123**, 174101 (2005).
[100] M. Shishkin, M. Marsman, and G. Kresse, Phys. Rev. Lett. **99**, 246403 (2007).
[101] M. Gerosa, C. E. Bottani, L. Caramella, G. Onida, C. Di Valentin, and G. Pacchioni, Phys. Rev. B **91**, 155201 (2015).
[102] K. J. Chang and M. L. Cohen, Phys. Rev. B **30**, 4774 (1984).
[103] D. M. Roessler and W. C. Walker, Phys. Rev. **159**, 733 (1967).
[104] R. Whited, C. J. Flaten, and W. Walker, Solid State Commun. **13**, 1903 (1973).
[105] J. E. Jaffe and A. C. Hess, Phys. Rev. B **48**, 7903 (1993).
[106] A. Ashrafi and C. Jagadish, J. Appl. Phys. **102**, 071101 (2007).
[107] H. Kumano, A. Ashrafi, A. Ueta, A. Avramescu, and I. Suemune, J. Cryst. Growth **214-215**, 280 (2000).
[108] S.-K. Kim, S.-Y. Jeong, and C.-R. Cho, Appl. Phys. Lett. **82**, 562 (2003).
[109] G. Lee, T. Kawazoe, and M. Ohtsu, Appl. Surf. Sci. **239**, 394 (2005).
[110] Y.-Z. Yoo, Y. Osaka, T. Fukumura, Z. Jin, M. Kawasaki, H. Koinuma, T. Chikyow, P. Ahmet, A. Setoguchi, and S. F. Chichibu, Appl. Phys. Lett. **78**, 616 (2001).